

# An Empirical Functional Representation, Extrapolation, and Internal Consistency of Second Virial Coefficients<sup>†</sup>

Gustavo A. Iglesias-Silva\* and Ruy Tellez-Morales

Departamento de Ingeniería Química, Instituto Tecnológico de Celaya, Celaya, Guanajuato, C.P. 38010, México

Mariana Ramos-Estrada

Facultad de Ingeniería Química, Universidad Michoacana de San Nicolás de Hidalgo, Morelia, Michoacán, C.P. 58060, México

Kenneth R. Hall

Chemical Engineering Department, Texas A&M University, College Station, Texas 77843

In this work, we present a simple pseudolinear function to extrapolate second virial coefficients to high temperatures or to correlate them using a Boyle temperature function. Accurate values of the Boyle temperature also result from this function if they are not available from measurement. With the new function, only two experimental points are necessary to predict the second virial coefficient within experimental error over a wide range of temperatures. The new approach is valid for pure and mixture second virial coefficients, and it provides a means to check the internal consistency among data using the Boyle temperature as a reducing parameter. Also, it allows simple representations of the second virial coefficient from pair potentials. It can be considered a tool to check the correct behavior of equations of state.

## Introduction

The virial equation of state when truncated after the second coefficient provides reliable values of the compression factor,  $Z$ , up to about a pressure equal to one-half the reduced temperature with an uncertainty of  $\pm 0.003$ . Under these circumstances, the virial equation of state becomes:

$$Z = \frac{P}{\rho RT} = 1 + B\rho \quad (1)$$

where  $P$  is the total pressure,  $T$  is the temperature,  $\rho$  is the molar density, and  $B$  is the second virial coefficient. The extension of eq 1 to mixtures is rigorous, and the second virial coefficient for an  $n$  component mixture is:

$$B_m = \sum_{i=1}^n \sum_{j=1}^n y_i y_j B_{ij} \quad (2)$$

where  $y_i$  are the mole fractions and  $B_{ii}$  and  $B_{ij}$  are the pure and cross second virial coefficients, respectively. Equations 1 and 2 can be used to calculate fugacity coefficients, densities, and other derived thermodynamic properties if the pure and cross second virial coefficients are available.

Unfortunately, the pure and cross second virial coefficients are not always available. To overcome this problem, these coefficients must be determined experimentally or predicted using a correlation. Naturally, the latter procedure is preferable because it takes less time and is less expensive. Numerous

correlations for pure and cross second virial coefficients have appeared in the literature; one of most widely used being that of Tsonopolous.<sup>1</sup> This corresponding states correlation uses the acentric factor and the critical pressure and temperature as characteristic parameters for simple molecules. More complex compounds, such as polar molecules, require a reduced dipole moment and constants for specific groups of molecules as well as different temperature functions.

Although the correlations for pure and cross second virial coefficients do a reasonably good job of predicting the virial coefficients at normal temperatures, they tend to fail at low temperatures for nonpolar and weakly polar molecules. The correlations are not as successful for strongly polar and associating substances.

In this work, we present an equation that can extrapolate the pure and cross second virial coefficients to high temperatures. The principal advantage of the new equation is that it is a simple linear function (for which the constants can be determined using two data points) that can predict the second virial coefficient within experimental error.

## Development

The corresponding states principle has supplied predictive equations for many thermodynamic properties, among them the second virial coefficients for pure substances. The reduced second virial coefficient is a summation of several terms:

$$B^*(T/T_c) = B_{\text{nonpolar,spherical}}^* + \omega B_{\text{non-polar,nonspherical}}^* + \mu^* B_{\text{polar}}^* + \dots \quad (3)$$

In general, eq 3 requires the critical pressure and temperature and the reduced temperature,  $T/T_c$ . Examples of such correlations

<sup>†</sup> Part of the "Sir John S. Rowlinson Festschrift".

\* Corresponding author. E-mail: gais@iqcelaya.itc.mx.

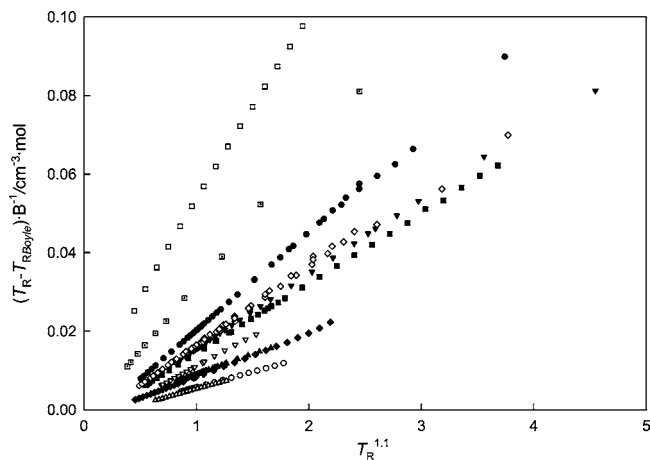


**Figure 1.** Linear behavior of the reduced second virial coefficient: ●, Ar; ▼, N<sub>2</sub>; ■, CH<sub>4</sub>; ▲, C<sub>2</sub>H<sub>4</sub>; ◆, C<sub>2</sub>H<sub>6</sub>; ○, C<sub>3</sub>H<sub>8</sub>; ▽, CO<sub>2</sub>; □, He; △, R-12; ◇, Kr; ◻, H<sub>2</sub>.

appear in Reid et al.<sup>2</sup> and Walas.<sup>3</sup> Some correlations attempt to use different dimensionless variables.

The Boyle temperature is the temperature at which the second virial coefficient becomes zero, that is:

$$B = B(T) = 0 \quad \text{when} \quad T = T_{\text{Boyle}} \quad (4)$$

At this temperature, the gas behaves more nearly like an ideal gas because  $Z = 1 + O(\rho^2)$ , and the contribution of higher terms may be negligible. The curve at which the compression factor equals unity is the Zeno line or the Boyle line. Several applications use this curve and this temperature to predict the Boyle temperature when it is not known experimentally, as by Wagner et al.,<sup>4</sup> to estimate the third virial coefficient at this temperature and the interrelationships among virial coefficients as in Holleran<sup>5</sup> and to predict rectilinear diameters and triple-point densities as by Ben-Amotz and Herschbach.<sup>6</sup>

In this work, we use the reduced Boyle temperature as a normalizing variable. As shown in Figure 1, plotting  $(T - T_{\text{Boyle}})/BT_c$  as a function of the reduced temperature results in a straight line:

$$\frac{T - T_{\text{Boyle}}}{BT_c} = k_1 + k_2 \left( \frac{T}{T_c} \right)^n \quad (5)$$

We have found that the exponent  $n$  is equal to 1.1 for most substances (even for substances with quantum effects, such as hydrogen, helium, and neon).

### Cross Second Virial Coefficients

If we define a cross Boyle temperature as the temperature at which the cross second virial coefficient becomes zero, then eq 5 becomes

$$\frac{T - T_{\text{Boyle},12}}{BT_{c,12}} = k_1 + k_2 \left( \frac{T}{T_{c,12}} \right)^n \quad (6)$$

where  $T_{c,12}$  is the cross critical temperature; in this work we use:

$$T_{c,12} = \sqrt{T_{c,11} T_{c,22}} \quad (7)$$

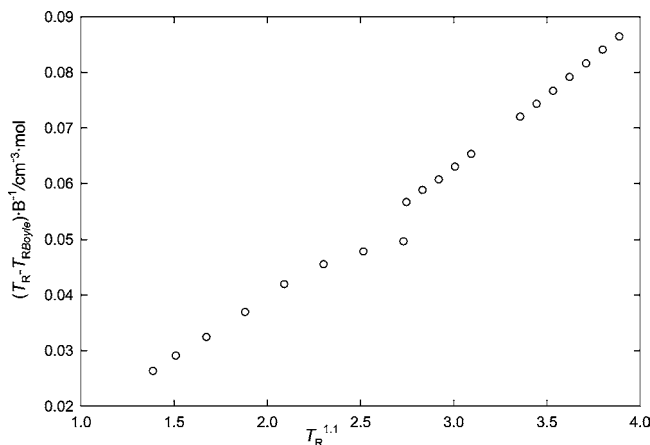


**Figure 2.** Linear behavior of the reduced cross second virial coefficient for nitrogen + oxygen.

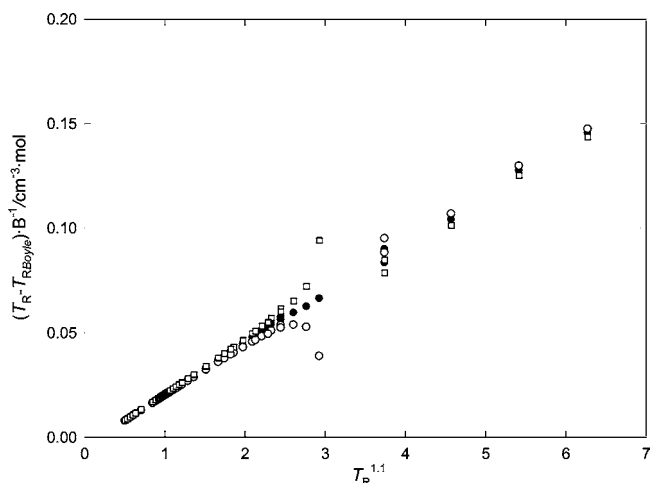


**Figure 3.** Effect of the Boyle temperature on the linearity of the reduced second virial coefficient: ●, Boyle temperature; ◻, Boyle temperature minus 5 K; ○, Boyle temperature plus 5 K.

The exponent  $n$  in eq 6 remains 1.1 for the mixtures treated in this work. Figure 2 shows the linear behavior for the system N<sub>2</sub> + O<sub>2</sub>. Experimental measurements come from Hall and Iglesias-Silva.<sup>7</sup> The main disadvantage of eqs 5 and 6 is that they do not satisfy the correct limit at low temperature, but it is an adequate expression to extrapolate the data to high temperatures, to show internal consistency among data sets and to find Boyle temperatures.

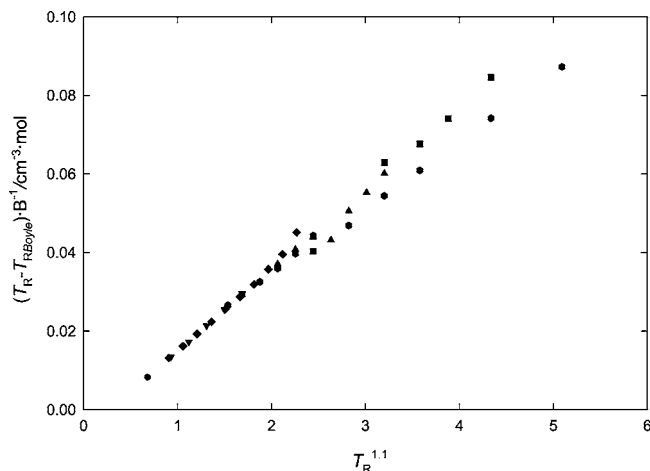
### Results and Discussion

**Calculation of the Boyle Temperature.** The Boyle temperature can be calculated from experimental measurements of pure and cross second virial coefficients or from an extrapolation of the Zeno line using pairs of  $T$  and  $\rho$  for which  $Z = 1$  and extrapolating to zero density. In this work, we propose to calculate the Boyle temperature by adjusting  $T_{\text{Boyle}}$  such that eq 5 is satisfied. If the Boyle temperature is not correct, a pole appears in a plot of eq 5. When the temperature is smaller than the true value, the left branch of the line tends to minus infinity, and if temperature is larger than the true value, the left branch of the line tends to plus infinity. Figure 3 shows this behavior for argon.

Table 1 compares the Boyle temperatures calculated using the current procedure to values obtained using other procedures. Boyle temperatures obtained from the Zeno line come from Ben-Amotz and Herschbach<sup>6</sup> and Xu and Herschbach.<sup>8</sup> We also have

**Table 1. Comparison of Boyle Temperatures for Pure Substances**

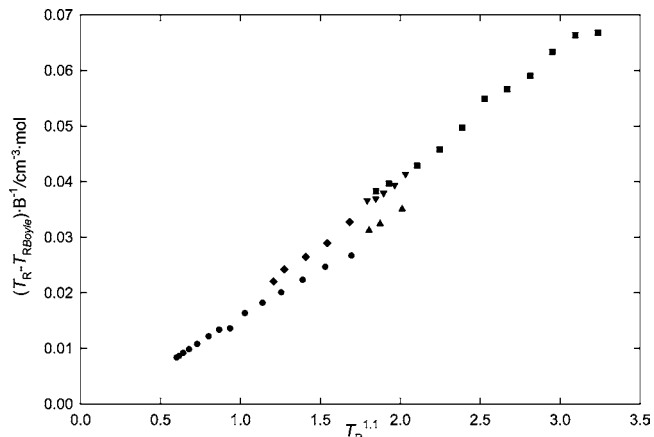
substance	$T_c/K$	$\omega$	$T_{Boyle}/K$	$T_{Boyle}/K$	$T_{Boyle}/K$
			this work	fit	Zeno line <sup>38</sup>
argon	150.663	0.000	412.00	412.51	408.35
neon	44.400	-0.029	122.60	122.86	120.32
krypton	209.400	0.005	580.00	580.21	569.61
xenon	289.700	0.008	775.00		792.81
nitrogen	126.193	0.037	326.80	326.88	326.41
oxygen	154.581	0.022	406.50	406.35	408.35
methane	190.551	0.011	508.65	508.82	509.74
ethylene	282.345	0.087	681.26 <sup>a</sup>		724.33
ethane	305.420	0.100	757.07 <sup>a</sup>		768.49
propylene	365.570	0.141	891.44 <sup>a</sup>		886.38
propane	369.850	0.153	891.66 <sup>a</sup>		902.56
<i>n</i> -butane	425.140	0.200	1003.51 <sup>a</sup>		1017.7
<i>n</i> -pentane	469.690	0.251	1081.63 <sup>a</sup>		1113.5
<i>n</i> -hexane	507.82	0.299			1185.5
<i>n</i> -heptane	540.13	0.349			1252.3
<i>n</i> -octane	569.32	0.393			1311.6
benzene	562.160	0.212	1347.03 <sup>a</sup>		1340.30
carbon dioxide	304.136	0.228	702.05 <sup>a</sup>		717.93
carbon monoxide	132.750	0.066	342.50	344.75	341.32
helium	5.190	-0.365	22.48	22.510	22.58
hydrogen	33.200	-0.218	107.30	111.16	109.43
deuterium	38.35	-0.148	113.55	113.92	
R12	384.950	0.186	929.26		929.69
R14	227.51	0.179			518.22
R23	299.29	0.263			717.29
R32	351.26	0.277			859.24
R41	317.28	0.2004			818.81
R123	456.83	0.282			1068.6
R124	395.43	0.288			926.63
R125	339.17	0.305			772.85
R134a	374.21	0.327			875.33
R141b	477.5	0.220			1141.2
R142b	410.26	0.232			982.17
R143a	345.86	0.262			833.59
R152a	374.21	0.275			875.33
methanol	512.6	0.563			1094.7
ethanol	513.93	0.644			1283.9
1-propanol	536.7	0.623			1435.6
ammonia	405.4	0.256			1034.78
water	647.1	0.344			1599.6

<sup>a</sup> Extrapolation using linear plots.**Figure 4.** Reduced second virial coefficient of carbon monoxide:  $\blacktriangle$ , Michels et al.;<sup>10</sup>  $\bullet$ , Mathot et al.;<sup>11</sup>  $\blacksquare$ , Collony;<sup>12</sup>  $\blacktriangledown$ , Brewer;<sup>13</sup>  $\blacklozenge$ , Goodwin;<sup>14</sup>  $\bullet$ , Deming and Shupe.<sup>15</sup>

calculated Boyle temperatures using eq 4 by fitting a second-degree polynomial to experimental second virial coefficients in the vicinity of  $B = 0$ .

#### Internal Consistency among Experimental Measurements.

The new procedure provides a consistency check for experimental data collected by different authors. The linear plot

**Figure 5.** Internal inconsistency between different data sets of the reduced cross second virial coefficient of nitrogen + methane. Data sets:  $\bullet$ , Byrne et al.;<sup>16</sup>  $\blacktriangledown$ , Lichtenhaler and Schaefer;<sup>17</sup>  $\blacksquare$ , Stein et al.;<sup>18</sup>  $\blacklozenge$ , Hahn et al.;<sup>19</sup>  $\blacktriangle$ , Martin et al.<sup>20</sup>**Table 2. Parameters Used in Equation 5 and Average Deviation of Equation 5 from Experimental Measurements**

substance/system	$T_{max}/K$	$k_1 \cdot 10^3$	$k_2 \cdot 10^2$	$\Delta B$	$\max  \Delta B $
		$cm^{-3} \cdot mol$	$cm^{-3} \cdot mol$	$cm^3 \cdot mol^{-1}$	$cm^3 \cdot mol^{-1}$
Pure Substances					
argon	1220	-4.5933	2.48579	0.27	1.96
neon	973	-5.0509	4.42284	0.22	0.65
krypton	715	-3.8876	0.02040	0.93	3.84
xenon	650	-2.8064	1.49419	0.68	4.11
nitrogen	700	-3.5714	1.90814	0.20	2.36
oxygen	300	-4.2663	2.31736	0.39	1.05
methane	623	-3.4340	1.78117	0.25	2.84
ethylene	450	-2.1674	1.11597	0.49	2.01
ethane	623	-2.3154	1.06575	0.76	3.78
propylene	560	-2.3946	0.88487	0.62	3.35
propane	623	-1.9727	0.77199	0.34	0.93
<i>n</i> -butane	573	-1.6891	0.59170	2.16	6.91
<i>n</i> -pentane	600	-1.5388	0.48464	4.45	14.70
<i>n</i> -hexane	600	-1.4938	0.42738	10.97	56.07
<i>n</i> -heptane	623	-1.2788	0.35480	6.28	27.62
<i>n</i> -octane	623	-0.9704	0.28159	32.01	74.37
benzene	623	-1.8977	0.62112	3.40	6.64
carbon dioxide	873	-4.6015	1.57092	0.39	2.15
carbon monoxide	573	-3.3437	1.83818	0.56	2.47
helium	1400	+2.9529	5.03210	0.71	2.77
hydrogen	400	-2.1074	3.40466	0.53	1.62
deuterium	423	-4.5406	3.60628	0.40	1.40
R12	478	-2.5937	0.79167	2.26	9.57
R14	773	-2.3978	0.98355	0.68	2.93
R22	473	-3.1839	0.97072	2.80	15.51
R23	393	-4.5853	1.21320	2.10	7.98
R32	420	-4.9456	1.22962	5.41	17.37
R41	423	-6.2732	1.51912	1.80	7.19
R123	453	-1.7288	0.53647	6.63	11.68
R124	400	-2.1088	0.63401	2.07	4.76
R125	480	-2.8549	0.76104	3.44	36.3
R134a	473	-2.9607	0.78394	3.38	14.06
R141b	400	-1.8948	0.62633	7.85	16.66
R142b	410	-2.5040	0.73474	5.57	20.32
R143a	440	-2.9085	0.78830	1.11	3.44
R152a	473	-3.0566	0.77531	4.49	25.88
methanol ( $n = 1.8$ )	623	-2.5287	0.90036	29.81	345.01
ethanol	533	-8.2359	1.51091	8.60	76.63
1-propanol	573	-6.1038	1.21790	8.12	19.86
ammonia	598	-9.2326	2.29989	2.83	6.66
water ( $n = 1.8$ )	1173	-3.6685	2.14369	9.83	498.75

#### Binary Systems

Ar + CH <sub>4</sub>	493	-2.9071	2.21247	0.10	0.26
Ar + Kr	500	-10.0495	2.71767	0.14	0.69
Ar + CO	475	-8.9354	2.50259	0.86	2.22
Ar + C <sub>2</sub> H <sub>6</sub>	511	-0.4821	1.28890	1.46	8.34
Ar + Xe	695	-2.9053	2.07031	0.66	2.61
Ar + Ne	323	-5.5343	2.91731	0.17	0.45
CH <sub>4</sub> + H <sub>2</sub>	283	21.1942	2.87843	0.10	0.30
CH <sub>4</sub> + CF <sub>4</sub>	623	-1.6976	1.24508	0.09	0.38
CO + He	296	15.5820	2.04933	0.48	1.03
CO + Ne	273	-4.7034	2.81737	0.04	0.10
N <sub>2</sub> + Ne	323	15.3536	2.37652	0.24	0.82
N <sub>2</sub> + O <sub>2</sub>	480	-5.5820	2.26610	0.61	0.26

Table 3. Parameters Used in Equation 5 from Two Data Points and Average Deviation of Equation 5 from Experimental Measurements

substance/system	$T_1, T_2/\text{K}$	$T_{\text{max}}/\text{K}$	$k_1 \cdot 10^3$ $\text{cm}^{-3} \cdot \text{mol}$	$k_2 \cdot 10^2$ $\text{cm}^{-3} \cdot \text{mol}$	$\Delta B$ $\text{cm}^3 \cdot \text{mol}^{-1}$	$\frac{\max  \Delta B }{\text{cm}^3 \cdot \text{mol}^{-1}}$
Pure Substances						
argon	81, 85	1220	-4.6573	2.49713	0.39	2.05
neon	65, 91	873	+0.9676	3.96778	1.04	2.16
krypton	110, 112	715	-3.9507	2.05181	0.94	3.53
xenon	160, 170	650	-2.6870	1.47600	0.90	3.56
nitrogen	75, 80	700	-3.5151	1.90908	0.32	2.50
oxygen	105, 110	300	-4.3664	2.32245	0.45	3.27
methane	117, 121	623	-3.6650	1.82038	0.57	2.07
ethylene	205, 220	450	-2.3792	1.14142	0.72	2.64
ethane	180, 190	623	-2.3048	1.06293	0.94	4.49
propylene	298, 318	560	-2.2652	0.86910	1.12	4.17
propane	285, 300	623	-1.9468	0.76778	0.64	1.66
<i>n</i> -butane	275, 300	573	-1.7832	0.60563	3.42	7.98
<i>n</i> -pentane	306, 318	600	-1.5240	0.48082	4.14	18.39
<i>n</i> -hexane	303, 316	600	-1.6672	0.45919	29.3	85.7
<i>n</i> -heptane	349, 358	623	-1.2132	0.34428	9.92	38.35
<i>n</i> -octane	367, 375	623	-0.7705	0.24726	55.82	110.2
benzene	373, 398	623	-1.8037	0.60718	3.91	7.44
carbon dioxide	217, 220	873	-4.2354	1.51926	1.19	2.69
carbon monoxide	120, 140	573	-3.1128	1.81352	0.57	2.61
helium	2.5, 3	1400	+0.0191	5.61792	1.32	3.15
hydrogen	14, 15	400	-1.9175	3.35610	0.61	1.86
deuterium	19, 20	423	-3.3569	3.35659	0.92	1.88
R12	255, 266	478	-2.5796	0.78437	3.34	6.48
R14	273, 298	773	-2.6641	1.01147	0.78	3.81
R22	233, 243	488	-3.1032	0.95781	2.85	16.10
R23	253, 263	393	-4.0836	1.15042	3.15	7.83
R32	210, 220	420	-4.4624	1.14154	13.71	23.10
R41	273, 297	423	-5.6994	1.45196	2.36	8.99
R123	290, 305	453	-1.6733	0.52537	8.64	17.25
R124	290, 300	400	-2.1372	0.63631	2.81	12.72
R125	280, 290	480	-2.4461	0.71651	3.13	11.84
R134a	245, 260	473	-2.6685	0.73831	9.61	15.91
R141b	270, 285	400	-1.5954	0.57002	23.24	41.89
R142b	248, 258	410	-2.1922	0.68078	13.13	31.42
R143a	276, 283	440	-3.0075	0.80064	1.46	3.84
R152a	233, 253	473	-2.9119	0.75040	8.03	31.38
methanol	357, 363	623	-2.6785	0.93530	35.15	560.56
ethanol	343, 353	533	-6.7774	1.29201	34.33	121.99
1-propanol	393, 408	573	-6.4246	1.26307	10.04	24.58
ammonia	253, 273	598	-8.5947	2.1918	4.45	6.94
water	303, 313	1173	-2.8830	1.84551	19.88	143.07
Binary Systems						
Ar + CH <sub>4</sub>	296, 308	493	+6.8768	1.69902	0.20	0.43
Ar + Kr	202, 213	500	-6.9003	2.44055	0.84	1.76
Ar + CO	213, 223	475	-34.1503	4.01311	1.15	2.99
Ar + C <sub>2</sub> H <sub>6</sub>	211, 231	511	-0.4086	1.28076	1.49	8.33
Ar + Xe	213, 233	695	-1.4181	1.95880	0.82	1.78
Ar + Ne	148, 173	323	-7.8105	3.43826	0.30	0.99
CH <sub>4</sub> + H <sub>2</sub>	144, 172	283	22.6632	2.82138	0.09	0.32
CH <sub>4</sub> + CF <sub>4</sub>	273, 298	623	-2.0741	1.26608	0.07	0.21
CO + He	77, 90	296	4.2601	2.17959	0.58	1.18
CO + Ne	123, 148	273	-4.0542	2.76226	0.05	0.14
N <sub>2</sub> + Ne	173, 198	323	7.0384	2.81815	0.69	1.69
N <sub>2</sub> + O <sub>2</sub>	188, 203	480	-4.891	2.2388	0.61	0.24

illustrates disagreements among experimental measurements even if the data are within the combined experimental uncertainties. The reduced second virial coefficients of carbon monoxide appear in Figure 4. We calculate a value of 342.5 K for the Boyle temperature for this substance. As shown in Figure 4, agreement exists among the measurements of Scott,<sup>9</sup> Michels et al.,<sup>10</sup> Mathot et al.,<sup>11</sup> Connolly,<sup>12</sup> Brewer,<sup>13</sup> and Goodwin.<sup>14</sup> However, the values measured by Deming and Shupe<sup>15</sup> are not consistent with the other values although their values overlap the other values within the estimated experimental errors.

For the system argon + methane, we have taken experimental values from Byrne et al.,<sup>16</sup> Lichtenhaler and Schäfer,<sup>17</sup> Strein et al.,<sup>18</sup> Hahn et al.,<sup>19</sup> and Martin et al.<sup>20</sup> The Boyle temperature calculated for this system is 433 K. When the experimental data

are plotted as a linear function, data from Martin et al.<sup>20</sup> and the high temperature values from Byrne et al.<sup>16</sup> are inconsistent with the rest of the experimental values. Figure 5 illustrates this behavior.

#### Correlation and Prediction of Second Virial Coefficients.

Equation 5 can both correlate and predict second virial coefficients. Table 2 demonstrates its performance as a correlating equation for several pure substances and binary systems. We have included nonpolar and polar substances. The polar substances are Freons, alcohols, and water. The exponent is different from 1.1 for alcohols and water. For water and methanol the exponent is 1.8. In all cases, we have to do a screening of the data due to the scatter in the measurements. The higher value of the exponent for water and methanol suggest that for polar substances the exponent can be different from

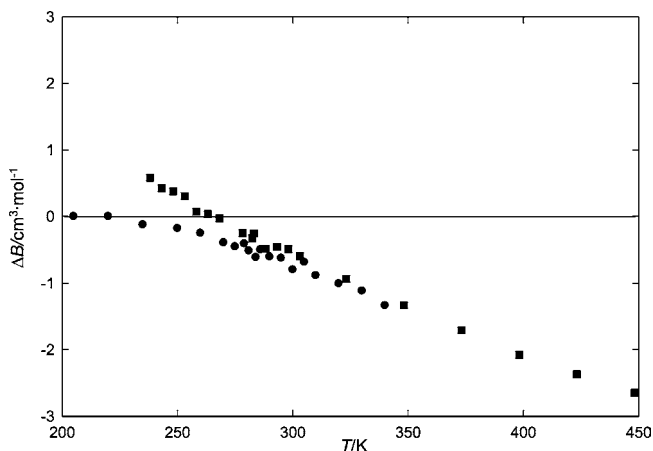


**Figure 6.** Extrapolation of eq 5 based upon two experimental points for ethylene: ●, Nowak et al.;<sup>21</sup> ■, Douslin and Harrison.<sup>39</sup>

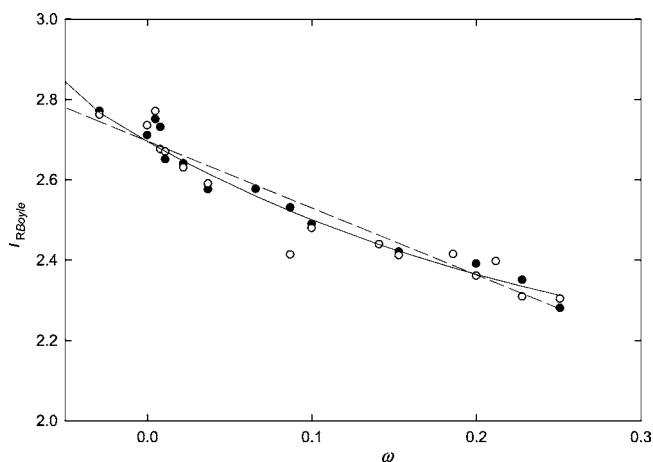


**Figure 7.** Boyle temperature for nonpolar substances. —, this work, eq 7; ---, Xu and Herschbach equation. Boyle temperatures: ●, Zeno line;<sup>6,8</sup> ○, this work.

1.1. However, when we curve-fit this parameter to the data we can find values slightly different from the suggested value, but if the value is fixed, the quality of the fit is as equally good as obtaining an optimum value. We tried to correlate the values of the exponent as a function of the reduced dipole moment, but we did not find a clean correlation; therefore, we decide not to report it at this time.

To test the validity of the linear assumption, we have used only two experimental data points for some substances. We have chosen, when reasonable, values at the two lowest temperatures because they represent a more stringent test being less reliable on average. Experimental measurements come from Nowak et al.,<sup>21,22</sup> Gupta and Eubank,<sup>23</sup> Gilgen et al.,<sup>24</sup> Dymond and Smith,<sup>25</sup> and Hall and Iglesias-Silva.<sup>7</sup> Table 3 provides the parameters  $k_1$  and  $k_2$ , the average absolute deviation, and the maximum absolute deviation.

In all cases, the extrapolation is outstanding considering that only two points have been used to develop the straight line. Figure 6 shows that the extrapolation for ethylene is within  $3 \text{ cm}^3 \cdot \text{mol}^{-1}$ . The Boyle temperature is calculated using the procedure suggested in this work, although the Boyle temperature from  $B = 0$  or from the Zeno line can be used. In the case of *n*-butane, the data from Gupta and Eubank<sup>23</sup> have been considered over the data from Ewing et al.<sup>26</sup> The experimental data from the former reference has better internal consistency than those from the latter reference. This result agrees with the conclusion reached by Tsonopolous and Dymond.<sup>27</sup>

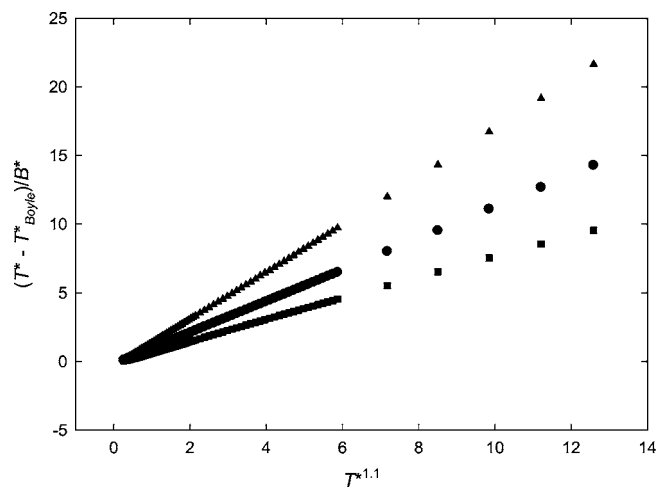


**Figure 8.** Linear behavior of the reduced second virial coefficient from different pair potentials. ●, Lennard-Jones; ■, square well; ▲, Buckingham (exp 6).

**Table 4. Comparison of Cross Boyle Temperatures**

system	$T_{c,12}/\text{K}$ eq 7	$T_{\text{Boyle},12}/\text{K}$ this work	$T_{\text{Boyle},12}/\text{K}$ eq 10
Ar + CH <sub>4</sub>	169.437	433	429.933
Ar + Kr	177.620	488	476.895
Ar + CO	141.503	393	386.617
Ar + C <sub>2</sub> H <sub>6</sub>	214.512	507	504.161
Ar + Xe	208.919	545	541.242
Ar + Ne	81.789	188	186.770
CH <sub>4</sub> + H <sub>2</sub>	79.538	203.7	207.162
CH <sub>4</sub> + CF <sub>4</sub>	208.253	466.9	475.331
CO + He	26.263	95	89.363
CO + Ne	76.816	171.1	169.467
N <sub>2</sub> + Ne	74.853	176.3	177.089
N <sub>2</sub> + O <sub>2</sub>	139.6	373.2	367.183

Sometimes, the Boyle temperature is not available experimentally. In this case, we have used a correlation<sup>28</sup> based upon the acentric factor:

$$T_{\text{Boyle}}/T_c = 2.0525 + 0.6428 \exp(-3.6167\omega) \quad (8)$$

Xu and Herschbach<sup>8</sup> also have developed an equation for the reduced Boyle temperature as a function of the acentric factor. We have not used their equation because it can predict negative Boyle temperatures for acentric factors greater than 1.62. Even though eq 8 has not been adjusted to the Boyle temperature of helium, it can predict that temperature within 1 K while Xu and Herschbach<sup>8</sup> underestimate it. Figure 7 shows the performance of eq 8 for nonpolar substances. For cross second virial coefficients, the Boyle temperature can be estimated using:

$$T_{\text{Boyle},12} = (T_{\text{Boyle},11} \cdot T_{\text{Boyle},22})^{1/2} \quad (9)$$

or from eq 8 as:

$$T_{\text{Boyle},12}/T_{c,12} = 2.0525 + 0.6428 \exp(-3.6167\omega_{12}) \quad (10)$$

with  $\omega_{12} = (\omega_{11} + \omega_{22})/2$  and eq 7.

**Table 5.** Expressions of  $(T - T_{\text{Boyle}})/(BT_c)$  from Different Equations of State

EOS	$\frac{T - T_{\text{Boyle}}}{BT_c}$
vdW	$\left(\frac{8P_c}{RT_c}\right)T_R$
D	$e^2T_R$
B	$\frac{T_R - \frac{3\sqrt{3}}{2\sqrt{2}}}{\frac{1}{8} \frac{RT_c}{P_c} \left(1 - \frac{27}{8} \frac{1}{T_R^2}\right)}$
RK	$\frac{T_R - \left(\frac{0.42748}{0.08664}\right)^{2/3}}{0.08664 \frac{RT_c}{P_c} \left(1 - \frac{0.42748}{0.08664} \frac{1}{T_R^{1.5}}\right)}$
SRK	$\frac{T_R - \left[\frac{1+m}{\left(\frac{0.08664}{0.42748}\right)^{0.5} + m}\right]^2}{0.08664 \frac{RT_c}{P_c} \left(1 - \frac{0.42748}{0.08664} \frac{1}{T_R} \eta\right)}$ $m = 0.48 + 1.574\omega - 0.176\omega^2$ $\eta = [1 + m(1 - T_R^{0.5})]^2$
PR	$\frac{T_R - \left[\frac{1+m}{\left(\frac{0.07780}{0.45724}\right)^{0.5} + m}\right]^2}{0.07780 \frac{RT_c}{P_c} \left(1 - \frac{0.45724}{0.07780} \frac{1}{T_R} \eta\right)}$ $m = 0.374644 + 1.5422\omega - 26992\omega^2$ $\eta = [1 + m(1 - T_R^{0.5})]^2$

Results from eq 10 appear in Table 4. For the substances treated in this work, prediction of the cross Boyle temperature from eq 10 is better than using the combinatorial rule.

**The  $(T - T_{\text{Boyle}})/(BT_c)$  Quantity from Equations of State and Pair Potentials.** We have obtained the  $(T - T_{\text{Boyle}})/(BT_c)$  quantity from different cubic equations of state (EOS): van der Waals (vdW), Redlich–Kwong (RK), Soave–Redlich–Kwong (SRK), Peng–Robinson (PR), Berthelot (B), and Dieterici (D). Table 5 presents the results for this quantity. It is interesting to notice that the vdW and D EOS are reduced temperature straight lines. We have also calculated this quantity using virial coefficients calculated from different pair potentials:<sup>29</sup> Lennard–Jones (6-12), modified Buckingham (6-exp), and the square-well potential as shown in Figure

8. From the second virial of the square-well potential, the  $(T^* - T_{\text{Boyle}}^*)/B^*$  quantity is

$$\frac{T^* - T_{\text{Boyle}}^*}{B^*} = \frac{T^* - \frac{1}{\ln\left(\frac{R^3}{R^3 - 1}\right)}}{1 - (R^3 - 1) \exp(1/T^*)} \quad (11)$$

where  $T^* = T/\varepsilon/k$  and  $B^* = (2/3)\pi N\sigma^3$ . Obviously, for all of the potentials, this quantity curves at the lower and higher temperatures. Botachev and Baidakov<sup>30</sup> suggested that most of the second virial coefficient data are in the temperature range of  $(0.5 - 3)T_c$  which corresponds approximately to a reduced temperature range of  $0.5 < T^* < 4.0$  for a Lennard–Jones fluid. We have considered the reduced temperature range of  $0.3 < T^* < 10.0$  and plotted the  $(T^* - T_{\text{Boyle}}^*)/B^*$  quantity versus  $T^{*1.1}$  for different second virial coefficients from different pair potentials. For the square-well potential, we use  $R = 1.5$ , while for the Buckingham (6-exp) we consider  $\alpha = 13.5$ . The linearity of the second virial coefficients from pair potentials is remarkable. To have a more stringent test, we have fitted the parameters of

$$\frac{T^* - T_{\text{Boyle}}^*}{B^*} = a + bT^{*k} \quad (12)$$

to the Lennard–Jones second virial coefficient obtaining  $a = -0.18619$ ,  $b = 1.13$ , and  $k = 1.1087$ . Next, we have fitted the parameters of the Lennard–Jones potential to experimental second virial coefficients and used those parameters in eq 12. The exponent is almost 1.1 as for the second virial coefficient experimental data. Figure 9 shows the residuals of the reduced second virial coefficient. Table 6 shows that there is a minimum deterioration of the evaluation of the second virial coefficient. Therefore a simple representation of the Lennard–Jones second virial coefficient is

$$B^* = \frac{T^* - 3.417928}{-0.18619 + 1.13T^{*1.1087}} \quad (13)$$

Equation 13 is only a representation of the second virial coefficient, and therefore it cannot be used to calculate derivatives accurately.

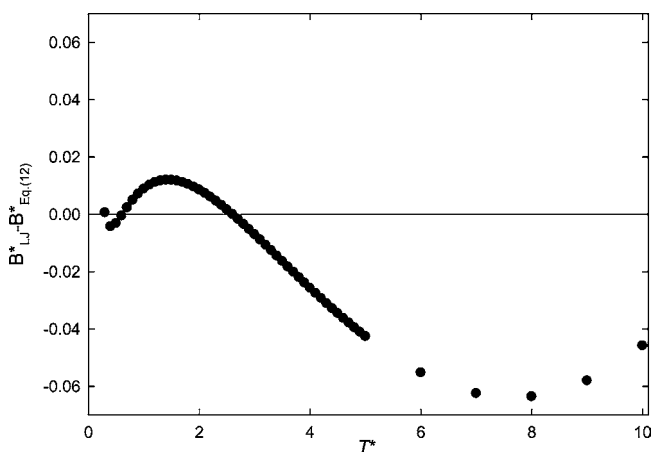


**Figure 9.** Difference between the Lennard–Jones second virial and those from eq 13.

**Table 6. Absolute Deviations from the Lennard–Jones Second Virial Coefficient and Equation 13 Using the LJ Parameters**

substance	$\sigma$ Å	$\epsilon/k$ K	$\Delta B_{LJ}$ cm <sup>3</sup> ·mol <sup>-1</sup>	$\Delta B$ , eq 12 cm <sup>3</sup> ·mol <sup>-1</sup>
argon	3.474	117.4	0.611	0.836
neon	2.7653	35.3452	0.132	0.158
krypton	3.9595	154.5	3.761	4.115
xenon	4.3567	204.7	2.383	2.741
nitrogen	3.8327	93.5858	1.891	2.140
oxygen	3.6122	114.4	2.079	2.237
carbon monoxide	3.8551	98.27	1.568	1.673
carbon dioxide	4.6858	181.5	5.350	5.406
methane	3.8499	147.20	0.683	0.874
ethane	4.8244	207.90	2.070	2.398
ethylene	4.8044	182.7	1.538	2.240
propane	6.1512	211.20	10.691	11.577
propylene	6.1965	195.30	4.098	4.422
<i>n</i> -butane	7.5505	206.80	15.294	16.032
isobutane	6.922	225.90	22.923	23.677
<i>n</i> -pentane	8.5599	219.90	33.066	33.947

Also this new representation can help in the development of the equation of state. For example, we have plotted the quantity  $(T - T_{Boyle})/(BT_c)$  versus  $T_R^n$  from different standard EOS (acetone,<sup>31</sup> argon,<sup>32</sup> ethanol,<sup>33</sup> methanol,<sup>34</sup> R134a,<sup>35</sup> and water<sup>36</sup>). As can be seen in Figure 10, some EOS do not follow the right behavior. Methanol and ethanol EOS have a curvature, one downward and the other upward. We have included for these two substances the recommended second virial coefficients<sup>37</sup> with the corresponding recommended uncertainty. Obviously, a straight line can pass through them within the given uncertainty. Therefore, this behavior can be used to correct these EOS. On the other hand, EOS for acetone, argon, R134a, and water follow linearity. These EOS have been plotted only in the temperature range where experimental data exist.

## Conclusions

We have presented a new approach to represent the second virial coefficients of pure substances and their mixtures. This new approach presents a simple, universal linear function that can be extrapolated within experimental error when the parameters of the equations are calculated using only two points at extreme conditions.

This new procedure also permits an accurate calculation of the Boyle temperature and can be used to check the internal consistency of experimental measurements or the consistencies

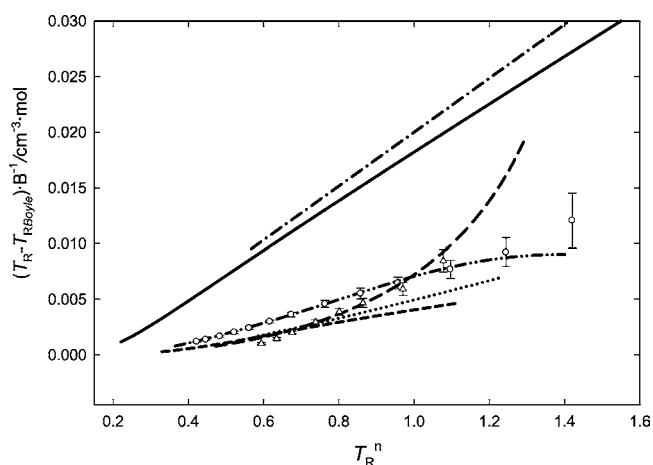


**Figure 10.** Behavior of  $(T - T_{Boyle})/BT_c$  from different EOS: ---, acetone;<sup>31</sup> - · -, argon;<sup>32</sup> —, ethanol;<sup>33</sup> · · ·, methanol;<sup>34</sup> · · ·, R134a;<sup>35</sup> - · -, water.<sup>36</sup> Recommended values:<sup>37</sup> Δ, ethanol; ○, methanol.

among different sets of data. We believe that this technique reduces the amount of data that need to be collected because only two points are necessary.

Also we believe this approach can be used as a constraint in the development of EOS. These variables can be used to represent the second virial coefficient even using pair potentials. This representation is not a substitute for existing correlations. It should be considered a tool to extrapolate and check the internal consistency of data and EOS.

## Literature Cited

- (1) Tsoupoloulos, C. An Empirical Correlation of Second Virial Coefficients. *AIChE J.* **1974**, *20*, 263–272.
- (2) Reid, R. C.; Prausnitz, J. M.; Poling, B. E. *The Properties of Gases and Liquids*; McGraw-Hill: New York, 1987.
- (3) Walas, S. M. *Phase Equilibria in Chemical Engineering*; Butterworth: Stoneham, MA, 1985.
- (4) Wagner, W.; Ewers, J.; Schmidt, R. An Equation of State for Oxygen Vapour-Second and Third Virial Coefficients. *Cryogenics* **1984**, *34*, 37–43.
- (5) Holleran, E. M. Interrelation of the virial coefficients. *J. Chem. Phys.* **1968**, *49*, 39–43.
- (6) Ben-Amotz, D.; Herschbach, D. R. Correlation of Zeno ( $Z = 1$ ) Line for Supercritical Fluids with Vapor-Liquid Rectilinear Diameters. *Isr. J. Chem.* **1990**, *30*, 59–68.
- (7) Hall, K. R.; Iglesias-Silva, G. A. Cross Second Virial Coefficients for the Systems  $N_2 + O_2$  and  $H_2 + O_2$ . *J. Chem. Eng. Data* **1994**, *39*, 873–875.
- (8) Xu, J.; Herschbach, D. R. Correlation of Zeno Line with Acentric Factor and Other Properties of Normal Fluids. *J. Phys. Chem.* **1992**, *96*, 2307–2312.
- (9) Scott, G. A. The Isotherms of Hydrogen, Carbon Monoxide and Their Mixtures. *Proc. R. Soc. London. A* **1929**, *125*, 330–344.
- (10) Michels, A.; Lupton, J. M.; Wassenaar, T.; de Graaff, W. Isotherms of Carbon Monoxide between 0 °C and 150 °C and at Pressures up to 3000 atm. *Physica* **1952**, *18*, 121–127.
- (11) Mathot, V.; Staveley, L. A. K.; Young, J. A.; Parsonage, N. G. Thermodynamic Properties of the System Methane + Carbon Monoxide at 90.67 K. *Trans. Faraday Soc.* **1956**, *52*, 1488–1500.
- (12) Connolly, J. F. The Virial Coefficients of Carbon Monoxide - Hydrocarbon Mixtures. *Phys. Fluids* **1964**, *7*, 1023–1025.
- (13) Brewer, J. Determination of Mixed Virial Coefficients, Report No. MRL-2915-C; Air Force Office of Scientific Research, No. 67-2795; Arlington, VA, 1967.
- (14) Goodwin, R. D. Carbon monoxide compressibility data from 100 to 300 K; derived virial coefficients, orthobaric densities, and heats of vaporization. *Cryogenics* **1983**, *23*, 403–414.
- (15) Deming, W. E.; Shupe, L. E. Some Physical Properties of Compressed Gases. II, Carbon Monoxide. *Phys. Rev.* **1931**, *38*, 2245–2264.
- (16) Byrne, M. A.; Jones, M. R.; Staveley, L. A. K. Second virial coefficients of argon, krypton and methane and their binary mixtures at low temperatures. *Trans. Faraday Soc.* **1968**, *64*, 1747–1756.
- (17) Lichtenthaler, R. N.; Schäfer, K. Intermolecular Forces of Spherical and Nonspherical Molecules Determined From Second Virial Coefficients. *Ber. Bunsenges. Phys. Chem.* **1969**, *73*, 42–48.
- (18) Strein, V. K.; Lichtenthaler, R. N.; Schramm, B.; Schäfer, K. Measurement of the Second Virial Coefficients of Some Saturated Hydrocarbons from 300–500 K. *Ber. Bunsenges. Phys. Chem.* **1971**, *75*, 1308–1313.
- (19) Hahn, R.; Schäfer, K.; Schramm, B. Measurements of the Second Virial Coefficients in the Temperature Range 200–300 K. *Ber. Bunsenges. Phys. Chem.* **1974**, *78*, 287–289.
- (20) Martin, M. L.; Trengove, R. D.; Harris, K. R.; Dunlop, P. J. Excess Second Virial Coefficients for Some Dilute Binary Gas Mixtures. *Aust. J. Chem.* **1982**, *35*, 1525–1529.
- (21) Nowak, P.; Kleinrahm, R.; Wagner, W. Measurement and correlation of the  $(p, \rho, T)$  relation of ethylene. I. The homogeneous gaseous and liquid regions in the temperature range from 105 to 340 K at pressures up to 12 MPa. *J. Chem. Thermodyn.* **1996**, *28*, 1423–1439.
- (22) Nowak, P.; Kleinrahm, R.; Wagner, W. Measurement and correlation of the  $(p, \rho, T)$  relation of nitrogen. I. The homogeneous gas and liquid regions in the temperature range from 66 to 340 K at pressures up to 12 MPa. *J. Chem. Thermodyn.* **1997**, *29*, 1137–1156.
- (23) Gupta, D.; Eubank, P. T. Density and Virial Coefficients of Gaseous Butane from 265 to 450 K at Pressures to 3.3 MPa. *J. Chem. Eng. Data* **1997**, *42*, 961–970.
- (24) Gilgen, R.; Kleinrahm, R.; Wagner, W. Measurement and correlation of the  $(p, \rho, T)$  relation of argon. I. The

- homogeneous gas and liquid regions in the temperature range from 90 to 340 K at pressures up to 12 MPa. *J. Chem. Thermodyn.* **1994**, *26*, 383–398.
- (25) Dymond, J. H.; Smith, E. B. *The Virial Coefficients of Pure Gases and Mixtures*; Oxford University Press: Oxford, 1980.
- (26) Ewing, M. B.; Goodwin, A. R. H.; McGlashan, M. L.; Trusler, J. P. M. Thermophysical properties of alkanes from speeds of sound determined using a spherical resonator 2. *n*-Butane. *J. Chem. Thermodyn.* **1988**, *20*, 243.
- (27) Tsionopoulos, C.; Dymond, J. H. Second virial coefficients of normal alkanes, linear 1-alkanols (and water), alkyl ethers, and their mixtures. *Fluid Phase Equilib.* **1997**, *133*, 11–34.
- (28) Iglesias-Silva, G. A.; Hall, K. R. An Equation for Prediction and/or Correlation of Second Virial Coefficients. *Ind. Eng. Chem. Res.* **2001**, *40*, 1968–1974.
- (29) Hirschfelder, J. O.; Curtiss, C. F.; Bird, R. B. *Molecular Theory of Gases and Liquids*; Wiley: New York, 1954.
- (30) Boltachev, G. S.; Baidakov, V. G. The Second and Third Virial Coefficients of Simple Fluids. *High Temperature* **2006**, *44*, 83–90.
- (31) Lemmon, E. W.; Span, R. Short Fundamental Equations of State for 20 Industrial Fluids. *J. Chem. Eng. Data* **2006**, *51*, 785–850.
- (32) Tegeler, Ch.; Span, R.; Wagner, W. A New Equation of State for Argon Covering the Fluid Region for Temperatures From the Melting Line to 700 K at Pressures up to 1000 MPa. *J. Phys. Chem. Ref. Data* **1999**, *28*, 779–850.
- (33) Dillon, H. E.; Penocello, S. G. A Fundamental equation for calculation of the thermodynamic properties of ethanol. *Int. J. Thermophys.* **2004**, *25*, 321–335.
- (34) de Reuck, K. M.; Craven, R. J. B. *Methanol, International Thermodynamic Tables of the Fluid State - 12. IUPAC*; Blackwell Scientific Publications: London, 1993.
- (35) Tillner-Roth, R.; Baehr, H. D. An International Standard Formulation for the Thermodynamic Properties of 1,1,1,2-Tetrafluoroethane (HFC-134a) for Temperatures from 170 to 455 K at Pressures up to 70 MPa. *J. Phys. Chem. Ref. Data* **1994**, *23*, 657–720.
- (36) Wagner, W.; Pruss, A. The IAPWS Formulation 1995 for the Thermodynamic Properties of Ordinary Water Substance for General and Scientific Use. *J. Phys. Chem. Ref. Data* **2002**, *31*, 387–535.
- (37) Dymond, J. H.; Marsh, K. N. *Virial Coefficients of Pure Gases and Mixtures*; Springer-Verlag: Berlin, 2002.
- (38) Estrada-Torres, R.; Iglesias-Silva, G. A.; Ramos-Estrada, M.; Hall, K. R. Boyle temperature for pure substances. *Fluid Phase Equilib.* **2007**, *270*, 148–154.
- (39) Douslin, D. R.; Harrison, R. H. Pressure, volume, temperature relations of ethylene. *J. Chem. Thermodyn.* **1976**, *8*, 301–330.

Received for review May 11, 2010. Accepted June 23, 2010. The Texas Engineering Experiment Station and the Instituto Tecnológico de Celaya have provided financial support for this work. ITC provided support through the Cuerpos Académicos Funding.

JE1004998